"The Impact of Blasting on Excavation Design - A Geomechanics Approach"

by

Patrick Andrieux, Noranda Technology Centre, Pointe-Claire, Quebec, Canada.
Cameron McKenzie, Blastronics (Australia) Pty. Ltd., Brisbane, Queensland, Australia.
John Heilig, BLM Blastronics Canada Ltd., Sudbury, Ontario, Canada, and,
Andrée Drolet, Noranda Technology Centre, Pointe-Claire, Quebec, Canada.

Abstract

It is widely accepted that both underground and surface blasting operations can de-stabilise excavations to the point where it can threaten the feasibility of mining through personnel safety or ore dilution. Research has been undertaken to outline a practical method in which the impact of blasting will be accounted for during the early excavation design stage by modelling, and during the following production stages by monitoring rock response to blasting operations.

Of the many factors influencing the stability of excavations in rock, a critical one is the natural geological structure. Given sufficient information about it (such as joint spacings, dips, orientations and strength index), excavations can be designed with high safety factors. However, if the natural structural state changes due to the passage of time or external influences such as blasting, safety factors may decrease, eventually leading to wall failures. The research work presented in this paper is part of a major effort aimed at integrating blast design with this aspect of rock mechanics excavation design. The chosen approach considers vibrations to be the primary cause for blast-induced rock damage in underground operations, where it is argued that gas effects have a lesser impact due to the usually high stresses confining fractures. The basis of the research consists of associating vibrations with fractures.

Tests were conducted during the Fall of 1992 in an underground experimental drift surrounded by two tunnels designed for observation and instrumentation purposes. A total of five rounds were blasted in the experimental drift; each time the blast design was altered to increase the amount of damage in the test tunnel, which was then observed and quantified from the observation drifts. Analysis of the results focused on establishing a relationship between vibration levels and the extent or degree of fracturing induced.

Other practical indirect measurement methods for assessing the extent of fractures in the rock mass, such as high frequency seismic methods, high resolution displacement analysis using a time domain reflectometry (TDR) method, and radar mapping, were also studied by the multi-disciplinary research team.

Introduction

A four-year major research program on blast-induced damage and its effects on excavation stability is currently being conducted by a Canadian mining industry consortium. Noranda, Inco, Falconbridge, Placer-Dome and Lac Minerals are partners in this joint venture financed through the Mining Research Directorate of Sudbury. The overall objective of this program is to develop a practical method to account, right from the early excavation design phase, for the effects blasting operations have on wall stability and ore dilution.

Field work for the second phase of this research program was conducted in November and December of 1992 at the Canada Centre for Mineral and Energy Technology (CANMET) experimental underground mine in Val d'Or, Quebec, Canada. The multi-disciplinary research team consisted of scientists from the Brisbane-based Blastronics (Australia) Pty. Ltd. firm; from BLM Blastronics Canada Ltd., a company located in Sudbury; from the Montreal-based Noranda Technology Centre (NTC); and from the Sudbury Division of Inco Limited.

This paper presents the overall research approach, as well as the experimental set-ups and procedures for some of the experiments conducted during Phase II of the project. Results, data analysis and

practical implications from these experiments are also presented.

General objectives and research approach

Structural damage caused to a rock mass by blasting operations has the potential to de-stabilise excavations to the point where safety concerns and ore dilution can threaten the very feasibility of mining. Of the large number of factors influencing excavation stability in rock, the natural geological structure is a critical one. Given sufficient knowledge about it, such as joint spacings, dips and orientations, and strength index, excavations can be designed with high safety factors. However, should the natural jointing be altered by the passage of time or external influences such as blasting, designs well adapted to the original conditions may not be adequate anymore, possibly leading to instability, wall failures and dilution. The engineering of an excavation should therefore take into account the resulting structural state of the rock, which is comprised of the natural joints and of the blast-induced ones.

The chosen research approach considers blast-induced vibrations as the primary cause for blast damage in underground excavations where it is argued that gas effects play a lesser role because of the confining effect stress has on fractures. The overall objective of this research program is thus to quantitatively link blast-induced vibration levels to the generation and extension of cracks in the rock mass.

Because of the broad scope of this research, it has been broken up into four successive phases, which are as follows:

Phase I - This first experiment concentrated on the blasting aspect of the program, with less emphasis on blast damage. This work, conducted during the summer of 1991, led to the conclusions that blast-induced vibrations are representative of the amount of work performed by an explosive charge and that vibration amplitude is a significant parameter in blast monitoring [1].

Phase II - The second experiment was designed to establish a correlation between blast-induced vibration amplitudes and the alteration of the structural state in a rock mass, which is considered to be a good indicator of blast damage. Another objective of this work was to compare well established direct methods of measuring in-situ fracturing with indirect techniques that could potentially turn out to be more rigorous, less expensive, and easier and faster to use.

Phase III - The third experiment, completed in 1993, took the research to two full-scale underground production stopes. The main objectives were to validate the results of Phase II in various realistic underground production environments.

Phase IV - The last phase of the program, planned for completion in 1994, will concentrate on the detailed back-analysis of all the data collected during the three experimental phases. Also, the development of relationships between blast-induced damage, dilution and ground support requirements, for variable in-situ rock conditions, will be pursued.

The remainder of this paper pertains to work conducted during Phase II of the research program, and more specifically to the near-field monitoring of the blast-induced vibrations, the direct blast damage assessment studies using borehole camera logging, and the high frequency cross-hole seismic surveys done to indirectly assess the in-situ cracking state of the rock.

Experimental set-ups and procedures

Field work for Phase II of the program was conducted from November 9 to December 11, 1992, at the CANMET experimental underground mine in Val d'Or. This time was allocated as follows: one week of site preparation, three weeks of experimental blasting and data acquisition, and one week of post-blasting detailed structural assessment of the test site. Another week was spent at the site, early in 1993, to conduct a high frequency ground-probing radar survey.

The field tests were conducted in an experimental drift 70 m below surface. The rock type varied from a medium-coarse grain hard granodiorite to a porphyry. Small veins of quartz and localised dykes could be observed in the rock mass, although only small quartz veins were present in the immediate vicinity of the tests.

The natural in-situ jointing pattern was mostly very continuous, and chlorite infillings were present on the surface of some joints.

The test drift, in which blasting took place, was located on the same horizontal plane and 5 m away from a parallel development drift, and 15 m directly below another tunnel and parallel to it, as seen in Figure 1 below. Both these tunnels were driven specifically for the study and were used as observation and instrumentation drifts from which blast vibration monitoring and blast damage assessment operations could be conducted.

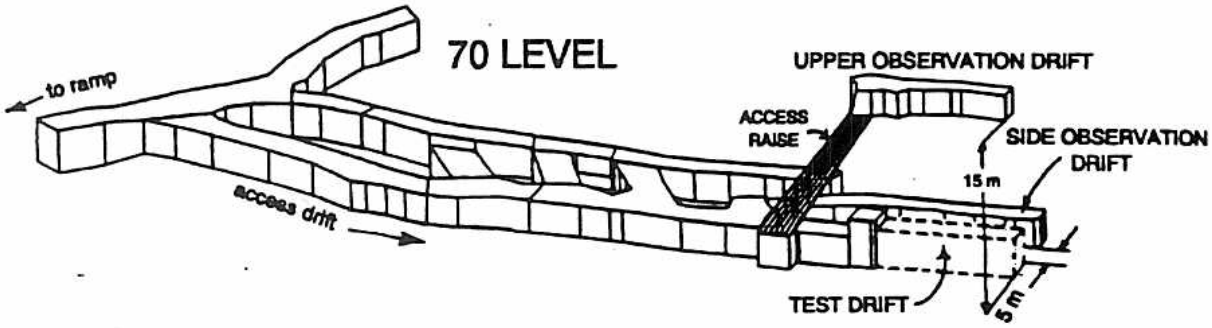

Figure 1 - Isometric view of the experimental site on Level 70, showing the test tunnel (in dashed lines), and both the side and the upper observation drifts.

Each of the five experimental rounds blasted in the test drift comprised two distinct blasts. The first one, always shot in the same manner, was simply aimed at removing an initial 1.5 m square by 2.5 m deep initial cut. This first blast was not instrumented and its sole purpose was to expose an inverted L-shaped 1.2 m thick skin of rock, as seen in Figure 2 below. This rock was then slashed in a second blast, which was fully monitored and studied. The slash was successively blasted harder and harder in order to increase damage to the adjacent rock. The muck produced by this slash was screened to give a precise idea of its fragmentation.

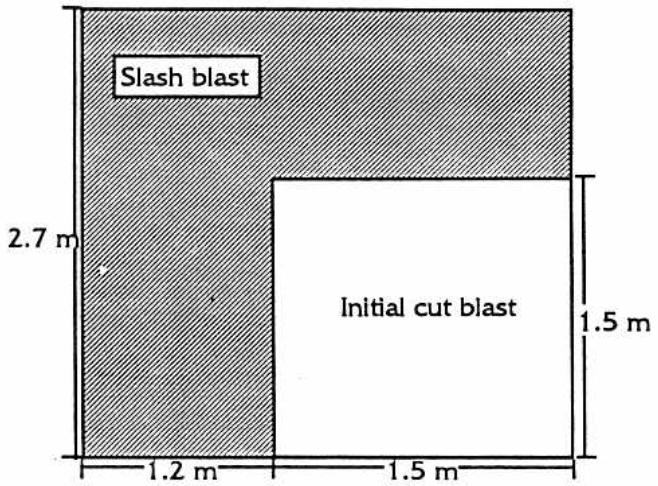

Figure 2 - Front view of the test drift showing the initial cut and the subsequent slash blast. The depth of each round was 2.5 m.

Each of the five series of experimental measurements was done using a dedicated array of instrumentation holes drilled from the upper tunnel, as seen in Figure 3 next page. For each array, five measurement holes were used; these were:

- One vertical 89 mm diameter percussion hole fitted with four sets of triaxial high frequency geophones located at 1.6, 3.1, 5.9 and 11.4 m from the planned final contour of the slash blast, in the back of the test drift. This arrangement was used to do vibration amplitude curve fitting in order to estimate amplitude levels at close vicinity to the blast, where most of the damage was anticipated. This hole was drilled vertically because

of the vibration transducers chosen. which had to be used either vertically or horizontally.

- One NQ size diamond drill hole dipping at 85 degrees for borehole camera logging. This hole was drilled at an angle to take advantage of the borehole camera's ability to directly map the observed features.
- Three 89 mm diameter percussion holes for ultra-sonic cross-hole seismic surveys. drilled so that their plane would include the NQ size borehole camera hole described above. (One of the objectives of Phase II was to compare cross-hole seismic survey results with the direct observation of cracks using the borehole camera: in order to do this. all these holes were located within the same plane.)

The collars of these instrumentation holes were located on different rings so that the "crack observation" plane would intersect the "blast vibration monitoring" plane about 2.3 m behind the planned back of the test drift. This was done in order to obtain maximum proximity between these planes. for correlation purposes. in the area close to the test drift. where it was anticipated the most relevant data were going to be.

Besides these blast-specific holes. a number of instrumentation set-ups were used for all five tests. Some of these also appear on Figure 3 and were as follows:

- Three horizontal NQ size diamond drill holes located parallel to the test drift (one in its centre. and one on each side. about a metre away from its final limits) for borehole camera logging along the axis of the tunnel.
- Two horizontal NQ size diamond drill holes located perpendicularly to the test drift. from the side observation tunnel. also for borehole camera logging. but of the other vertical plane.
- Five surface-mounted OYO GeoSpace 101 LT directional uniaxial high frequency geophones bonded directly to the wall of the side observation drift. and pointing toward the test tunnel.

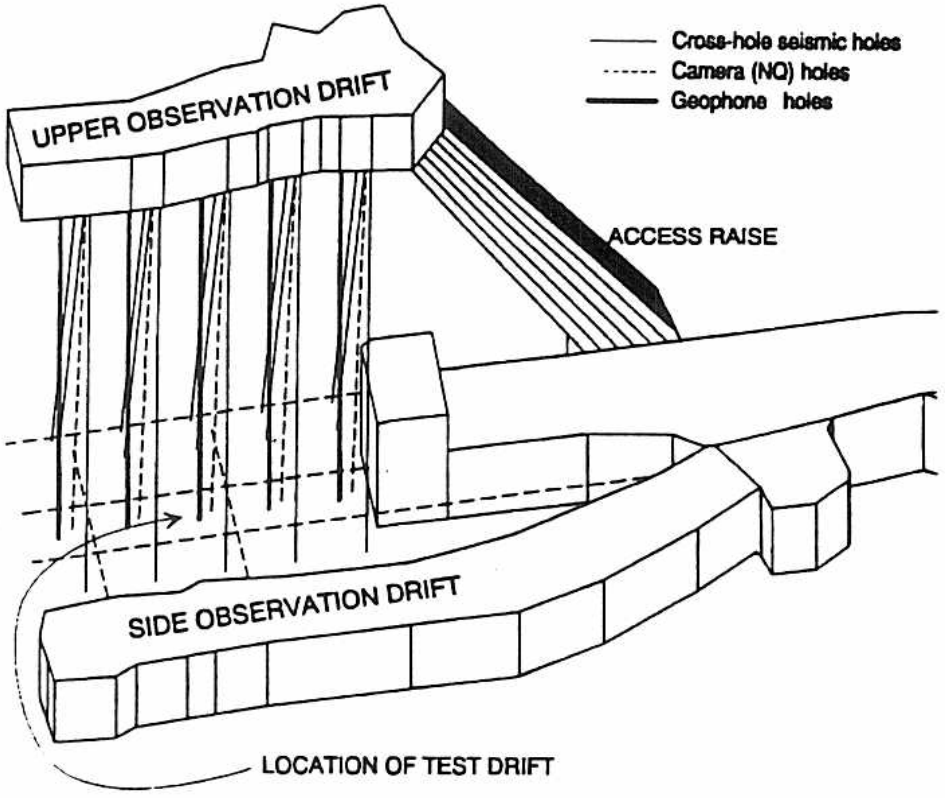

Figure 3 - Isometric view showing the instrumentation holes used for blast vibration monitoring, borehole camera logging and cross-hole seismic surveys.

Each blast vibration monitoring triaxial sensor installed in a geophone hole was comprised of three uniaxial OYO GeoSpace 101 LT directional high frequency McSeis type geophones mounted in an orthogonal manner in a plastic angle and shunted with 3900 Ω resistors. The plastic angle was inserted into a length of 51 mm diameter ABS pipe and encased in low curing temperature two-components araldyte epoxy. The four

triaxial sets used in each monitoring hole were connected together using 51 mm diameter ABS pipe cut to length and glued together. This setup allowed to maintain all the triaxial arrangements pointing toward the same chosen direction. Once the complete string of sensors was in place, the geophone hole was grouted and left curing for three days. One inch circular holes drilled along the ABS pipe every 50 cm allowed the grout to fill both the inside and the outside of the pipe, insuring tight coupling to the rock.

The geophones used had an average sensitivity of 0.035 Volt per mm/sec. In order to increase blast vibration monitoring accuracy, each transducer was calibrated relative to a sensor that had been calibrated in an absolute manner. Although this did not provide information on the frequency response of each sensor, it allowed to know precisely the sensitivity of each of the sixty-five sensors used, which varied by no more than 7% from their mean nominal sensitivity.

Full waveform blast vibration monitoring was performed using multi-channel digital seismographs, sampling at 50 kHz, which is ample speed considering geophones were used. Because at this sampling rate the recorders were limited in terms of recording duration, the slash blasts were all fired using CXA short period non-electrical XT detonators (numbers 1 to 18). A "wire-break" triggering method was used to synchronize the vibration measurements to the blasts.

As mentioned previously, direct fracture measurements were performed using diamond drill coring, face mapping, and a high resolution borehole camera. The objectives of these measurements were firstly to establish in-situ pre and post-blast rock conditions, and, secondly, to act as a reference against which results from the indirect observation techniques could be compared. Direct joint observation was systematically done before and after each slash blast to closely follow the evolution of cracking in the rock mass.

Figure 4 below shows the experimental arrangement used for each set of measurements for the blast vibration monitoring, the borehole camera mapping and the cross-hole seismic techniques. For the cross-hole seismics, of the three holes used on each ring, two were located on one side of the tunnel, 1 m apart and parallel to each other, while the third one was drilled on the other side of the tunnel, diverging from the previous two. The parallel hole located on the outside was the source hole, in which a pulse transmitter was lowered. This transmitter was a high frequency (centred at about 32 kHz) piezoelectric ultra-sonic source driven by a high voltage capacitor discharge. The other two holes were used as receptor holes (a high frequency B&K 8101 hydrophone was inserted in each of them). This set-up was used so the borehole near the source could act as a source reference, which made it possible to account for source variability.

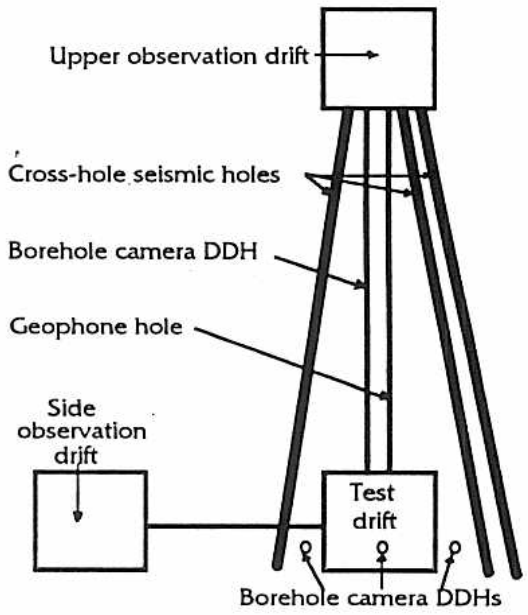

Figure 4 - Schematic front elevation view of one instrumentation ring, showing the three cross-hole seismic holes, the borehole camera diamond drill holes and the geophone hole. The dip of these holes can be seen in Figure 3. This setup was repeated five times (once per blast).

All three cross-hole seismic instruments (the source and the two hydrophones) were simultaneously lowered into their respective boreholes. Actual measurements consisted of recording the pulse emitted by the piezoelectric source with the two hydrophones, in order to quantify attenuation between the various points. At each depth down the holes, a hundred measurements were averaged to boost the signal to noise ratio. Scanning was conducted at 30 cm vertical intervals starting at the back of the excavation and finishing at about 5 m from it. All the cross-hole seismic instruments were coupled in water.

The other indirect measurement techniques used to study the evolution of the fractures in the rock mass were surface seismic surveys, high frequency radar studies and a time domain reflectometry (TDR) technique. The description of these methods and of their results are not presented in this paper.

Detailed conventional surveying was extensively performed during the entire duration of the tests. Surveying was done to obtain the collar location of each blasthole and of each instrumentation hole (these instrumentation holes were also surveyed using a borehole deviation survey instrument to measure their precise shapes and locations). Surveying was also used to obtain surface profiles before and after each blast: this allowed to assess the burden in front of each blasthole as well as the overbreak produced by each blast. All this survey data were imported into AutoCAD™, for easier display and manipulation.

Experimental results and data analysis

During the three weeks of field work, blasting of the five test slashes went from smooth (contour blasting in 32 mm blastholes, lightly confined), to hard (45 mm holes fired with high energy watergel on a larger burden) to very hard (57 mm blastholes highly confined and loaded with AnFO explosives) to smooth again. Table 1 below shows the design parameters for each of the five test slashes fired: for each blast the slash had the same dimension (width of 1.2 m along an L-shape, as seen in Figure 2). Damage to the rock mass was principally controlled by changing the confinement (burden) of the peripheral charges. This confinement varied from as little as 0.20 m to as much as 1.40 m. In order to differentiate between vibrations emitted by the different explosive charges detonated in a blast, each slash hole within each test blast was fired on its own detonator period.

Blast number	Hole diameter *(mm)*	Number of holes	Explosive types	Powder factor *(kg/m³)*
Blast #1	32	19	AnFO/Minerite2	2.20
Blast #2	45	11	Minerite2	1.70
Blast #3	57	7	AnFO	2.70
Blast #4	57	5	AnFO	2.70
Blast #5	32	20	Minerite2	4.70

Table 1 - Blast design parameters for each of the five slash blasts.

Blast vibration monitoring results and data analysis

The vibration traces recorded during the study permitted the determination of separate attenuation equations for each test round, using the Holmberg equation [2]. For the case of square root scaling, the Holmberg equation has an analytical solution which reduces the generic integral equation to the following:

$$PPV = K\,(I/Ro)^{\beta/2}\,[\phi - \arctan\{(Ro\tan\phi - H)/Ro\}]^{\beta/2} \quad \ldots\ldots\ldots (1)$$

With: PPV the peak particle velocity anticipated at the point of interest (in mm/sec), K and β two site specific constants, I the linear charge density (in kg/m), Ro the horizontal distance between the charge and the point of interest (in metres), ϕ the angle between the bottom of the charge and the point of interest (measured from the horizontal), and H the height of the charge (in metres).

The terms K and β of this equation were calculated independently for each test blast by regressing the recorded vibration data to obtain least square estimates for these values. Because each charge was detonated on its own detonator period, the vibration amplitude produced by each independent charge could be considered in the calculations. The peak particle velocities required to fit the data to the Holmberg equation were obtained

by using the following formula:

$$PPV(t) = [\ \{Vx(t)\}^2 + \{Vy(t)\}^2 + \{Vz(t)\}^2\ ]^{1/2} \quad \text{..... (2)}$$

With : PPV the peak particle velocity, Vx the vibration amplitude along the transversal direction, Vy the vibration amplitude along the longitudinal axis, and Vz the vibration amplitude along the vertical axis, all expressed in mm/sec, at instant t.

The actual PPV used in the Holmberg equation and quoted in the remainder of this paper is the maximum of this function, which physically represents the maximum instantaneous vector sum value of the three orthogonal components of the vibration. Using spreadsheet programs, the terms K and β were calculated, as well as the regression coefficient R. Results from these manipulations are presented in Table 2 below:

Blast number	Constant K	Constant β	Sample size	Coefficient R
Blast #1	1231	1.54	30	0.62
Blast #2	603	1.01	47	0.87
Blast #3	68024	3.51	14	0.72
Blast #4	878	0.90	24	0.75
Blast #5	527	1.35	40	0.80

Table 2 - Regression parameters for each of the five slash blasts.

Since the value of β is less than 1 for blast #4, the equation resulting from this data fitting can only be used with caution. Similarly, the abnormally high value of K obtained for blast #3 limits the reliability of this equation outside its own data set.

The effect of blasthole location was investigated to determine if it was adequately accounted for with the equations obtained. The charges located near the bottom half of the slash had the potential to be shielded from the geophones by the blasted void and therefore return non-representative lower vibration levels. To study this, the data were separated into two groups: one group related to the charges located above the halfway elevation of the round, and the other group related to the charges located below this mark. These two groups of data were plotted on the same PPV vs. distance graph. No definite trend could be seen which indicated that the equations provided the same degree of scatter when the data were separated according to the location of the charges.

Similarly, the data were analyzed to insure the equations properly took into account explosive charge weights. The explosive charge weights used during the study varied from 0.7 to 8.4 kg: to verify if the equations obtained adequately accounted for an order of magnitude variation in the charge weights, the data were separated into two groups about a charge weight of 1.7 kg. As for the previous case, when both groups were plotted on the same PPV vs. distance graph, no definite trend could be observed. These results gave good confidence that equation (1) provided a good estimate of vibration levels, and that the scatter observed was inherent to the experimental procedure.

A collective vibration equation was derived to predict PPV for situations outside the range over which the experimental data were collected. To obtain this single equation, all the data collected from the five test blasts were used in the regression process, regardless of the conditions in which it was obtained. For this new sample, K was calculated at 685, β was determined to be 1.12 and the associated regression coefficient R was 0.74. The collective equation obtained was thus as follows:

$$PPV = 685\ (l/Ro)^{0.56}\ [\phi - \arctan\ \{(Ro\ \tan\phi - H)\ /\ Ro\}]^{0.56} \quad \text{..... (3)}$$

To verify the ability of this equation to adequately describe all the data, it was assessed whether or not this collective regression line fell within the upper and lower bands statistically defined by each of the five data sets. Results from these statistical manipulations indicated that the collective regression equation described vibration data from blasts #1 and #2 with good accuracy. Blast #3 was not well described by the collective equation; however, the abnormally high values of K and β obtained from this data set intuitively lead to argue that the collective equation may not necessarily represent it more poorly. The collective equation described the data sets of blasts #4 and #5 sufficiently well to keep them in this collective equation.

Figure 5 next page shows how all the measured data compared to the 95% confidence level collective

vibration equation. This later equation was obtained by replacing the term K in the mean collective equation by the term K_{95} given by equation (4) below:

$$K_{95} = K_{mean} + t_{5\%}\ S_{(y,x)} \qquad \text{..... (4)}$$

With: K_{mean} the value of the mean collective equation constant, $t_{5\%}$ the value of the t Distribution at the 5% confidence level with n-2 degrees of freedom (with n the number of data points), and $S_{(y,x)}$ the estimated standard error of the y values.

The 95% confidence level collective equation was obtained with equation (4) by using $t_{5\%} = 1.65$, which gave a K_{95} of 1850. On Figure 5, the Holmberg Term appearing on the X axis is the following value:

$$\text{Holmberg Term} = (l/R_o)\ [\phi - \arctan\ \{(R_o \tan\phi - H) / R_o\}] \text{..... (5)}$$

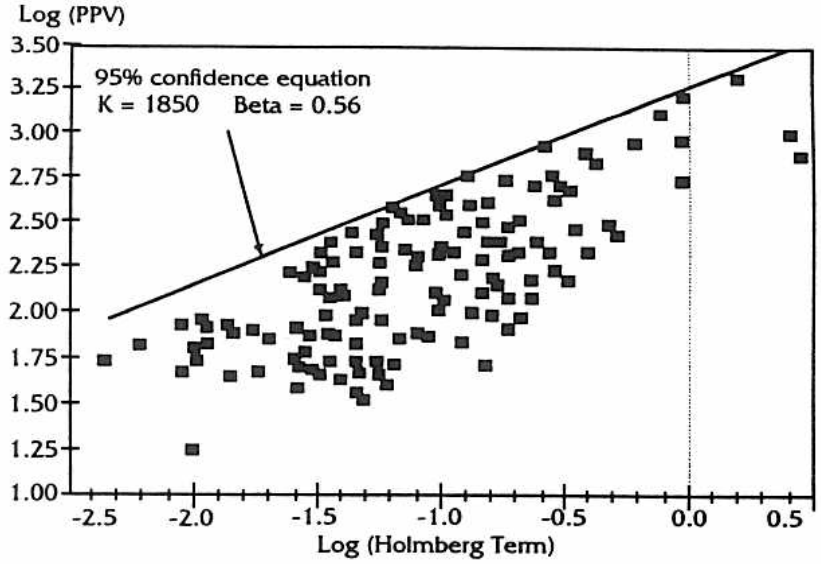

Figure 5 - Comparison of all the measured data with the 95% confidence level collective vibration equation.

Based on this statistical analysis, equation (3) was retained to evaluate vibration levels at various distances away from a charge (from 1 to 10 m) and for various explosive weights (up to 10 kg). This equation was needed to estimate vibration levels at points where blast damage was observed, in order to correlate the two.

Direct damage assessment

Direct damage assessment was done by surveying the fracture state of the rock mass before and after blasting. Prior to shooting any round, the initial fracture state in the test area was studied by detailed joint mapping in the two observation tunnels, borehole mapping in three orthogonal directions around the test drift and diamond drill core logging. Post-blast direct fracture assessment was only done by performing borehole camera surveys. Blast-induced overbreak was directly measured using high precision conventional surveying equipment and by comparing the final contour of the excavation after each slash blast with the location of the peripherical blastholes.

Direct damage assessment techniques allowed to identify three distinct types of blast-induced damage which were: overbreak, creation of new fractures and extension of previously existing fractures.

As mentioned, overbreak was directly measured even though its assessment was sometimes difficult to achieve because of the influence of small wedges, which could distort the results. Overbreak varied from 80 mm to 20 cm, depending whether or not smooth blasting was done; using equation (3) along with the charging and geometrical information for each blast, this range of overbreak corresponded to vibration levels of 3500 to 4500 mm/sec. Fresh fractures were generally not observed at distances greater than 1.5 m from the 57 mm diameter

blastholes and 80 cm from the 32 mm blastholes. These corresponded to vibration levels ranging from about 850 to 1000 mm/sec, according to equation (3). The extension of fractures, which pertains to both the extension and the opening of previously existing discontinuities, has been typically observed at distances no greater than 4.5 m away from the 57 mm blastholes and 3.5 m away from the 32 mm blastholes, which related, again using equation (3), to vibration levels varying from 300 to 400 mm/sec.

Cross-hole seismic survey results and data analysis

The principle on which cross-hole seismic surveys rest is that seismic pulses travelling through a rock mass will attenuate, causing a reduction in both the amplitude and the frequency content of the waves, with the amount of reduction increasing with increasing distance and with increasing jointing or fracturing. This sensitivity to rock structure makes the technique appealing for quantifying blast-induced damage. Cross-hole seismic scans were conducted before and after each slash blast in order to assess the deterioration of the rock mass caused by the generation and/or the extension of fractures in the matrix.

The first arrival pulse rise time τ is considered to give a good indication of the change in frequency of a propagating wave. Furthermore, the first arrival pulse amplitude is a good indicator of the change in amplitude in a seismic wave. The difficulty with both these measurements is that they should be conducted on un-distorted first arrivals, which are not necessarily encountered, especially when the rock condition is poor; in this case, first arrivals can be difficult to identify, even with signal averaging. Also, distortion of first arrivals is common due to the near-simultaneous arrival of several pulses. This is a significant problem because the most interesting areas (where blast-induced damage has taken place and could be observed) are also the most likely to produce hard to identify and distorted first arrivals. Because of these practical limitations in studying first arrival pulse rise times and amplitudes, the cross-hole seismic studies conducted in this project considered average amplitudes of the seismic waves as obtained by measuring the RMS amplitudes for the full 3 msec pulse duration.

Amplitude changes between the two receiver holes have been expressed in decibels, defined by equation (4) below:

$$dB = 20 \log_{10} (A_1 / A_2) \qquad \text{..... (4)}$$

With: dB the amplitude change between receivers 1 and 2, and A_1 and A_2 the Root Mean Square amplitudes measured at holes 1 and 2 respectively.

The difference in decibel levels between the pre-blast and the post-blast conditions were plotted for each test blast. Because of difficulties with the instrumentation, cross-hole seismic data were available only for blasts #1, #2, #3 and #5. Figure 6 below shows the results obtained for these pre and post-blast conditions.

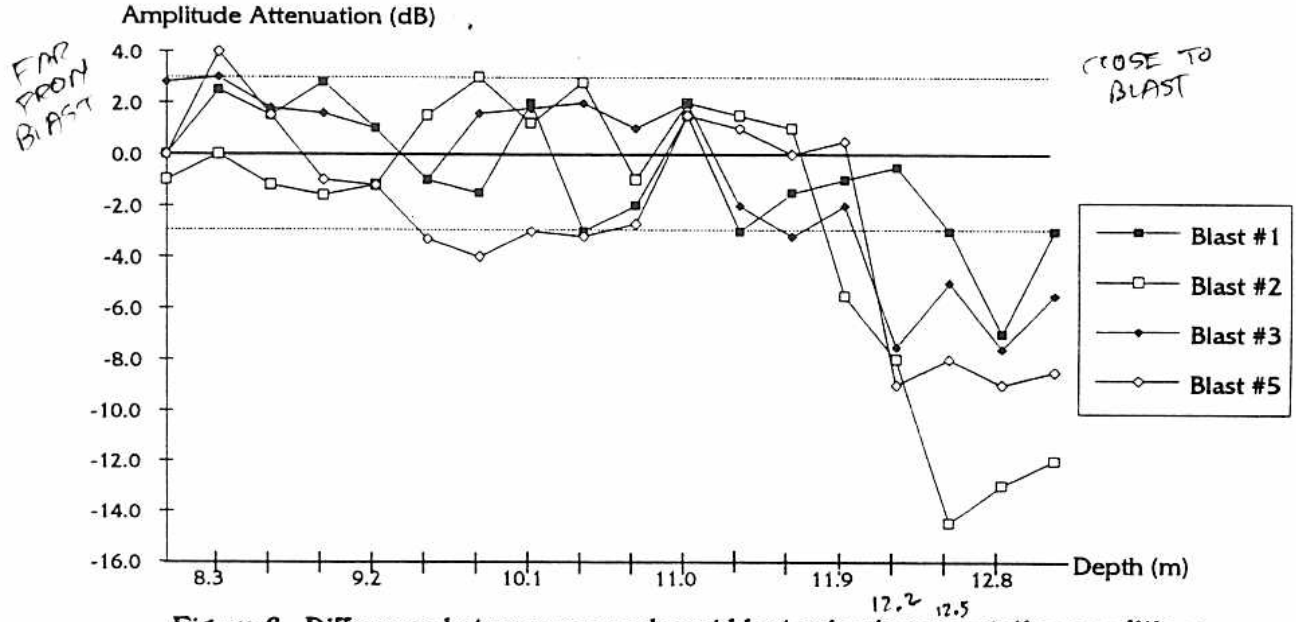

Figure 6 - Difference between pre and post-blast seismic propagation conditions.

Where little change between pre and post-blast conditions was encountered (i.e., where no or little blast damage took place), only a small change in signal amplitude (in dB) was observed. As blast-induced damage increased, thus increasing the difference between pre and post-blast conditions, the change in signal amplitude (again expressed in dB) also increased. Negative changes indicate a decrease in rock mass quality, while positive variations indicate an increase in rock quality.

As seen in Figure 6, changes in signal amplitude between pre and post-blast conditions were typically low (± 3 dB) on the upper portion of the scanned area, away from the blast. This ± 3 dB variation was considered to be experimental noise because it was unlikely that the rock mass was disturbed that far away from the test blasts. At a certain distance away from the blasts, the change in amplitude increased beyond the ± 3 dB limit and kept shifting toward the negative as the distance to the blast decreased, indicating a decrease in rock mass quality. The distance away from the blast at which the - 3 dB mark was passed was assumed to be the limit of blast damage; these distances are shown in Table 3.

Blast number	Blasthole diameter	Explosive type	Depth of damage	Depth of blastholes	Damage extent
Blast #1	32 mm	AnFO/Minerite2	12.5 m	13.2 m	700 mm
Blast #2	45 mm	Minerite2	11.7 m	12.7 m	1000 mm
Blast #3	57 mm	AnFO	11.5 m	12.7 m	1200 mm
Blast #4	57 mm	AnFO	–	–	–
Blast #5	32 mm	Minerite2	12.0 m	12.8 m	800 mm

Table 3 - Damage limits detected by the cross-hole seismic surveys.

As seen in Table 3, as blasting of the successive slashes went from gentle to hard, the extent of blast damage in the surrounding rock increased. When blasting became smooth again for blast #5, the extent of damage in the rock mass decreased.

Using equation (3), vibration amplitudes at the boundary of the damage zones suggested by the cross-hole seismic technique, could be evaluated for each case; these results are presented in Table 4 below.

Blast number	Damage extent	Estimated PPV
Blast #1	700 mm	860 mm/sec
Blast #2	1000 mm	890 mm/sec
Blast #3	1200 mm	1160 mm/sec
Blast #4	–	–
Blast #5	800 mm	930 mm/sec

Table 4 - Comparison of the extent of damage with the estimated maximum PPV generated.

Discussion and implications

Both the direct borehole camera mapping and the indirect ultra-sonic cross-hole seismic assessment techniques showed abilities to detect blast-induced damage in the rock matrix. Both methods were in reasonably good accordance as far as assessment of damage extent (i.e., the creation of new cracks) was concerned. In the rock type and conditions in which the study was conducted, the limit of fresh fracturing, as suggested by borehole camera studies in the case where blasting was the most violent, was about 1.5 m while the limit of damage, as assessed with the seismic method for the same blast, was around 1.2 m. For all the blasts, the vibration amplitudes corresponding to the onset of damage varied from 800 to 1500 mm/sec (as indicated by the borehole camera surveys) and from 800 to 1200 mm/sec (as suggested by the seismic technique). These values are not very far from the ones proposed by Holmberg & Persson (1979) for hard rock, which are 700 to 1000 mm/sec.

Theoretically, the peak particle velocity which could damage the rock can be calculated using the following equation:

$$PPV_{max} = V_p (\sigma_T / E) \qquad \text{..... (5)}$$

With: PPV_{max} the vibration amplitude at which tensile failure of the rock will occur (m/sec), V_p the p-wave velocity of the rock (m/sec), σ_T the rock strength (MPa) and E the Young's Modulus (MPa).

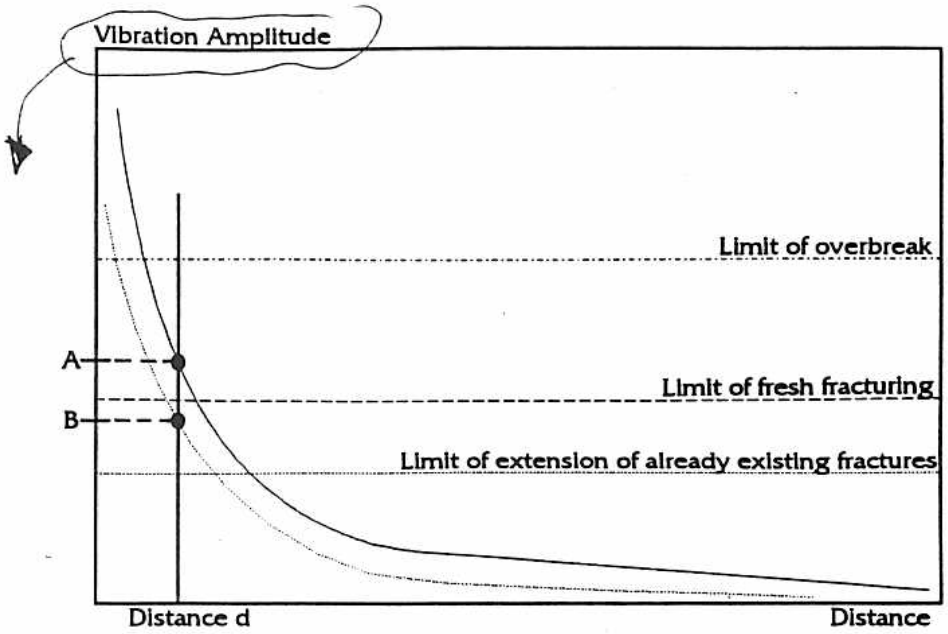

Figure 8 - Superimposition of a near-field vibration prediction equation and of the limits of the three types of blast-induced damage.

Let us assume that a delicate wall is located at a distance d away from the blast. At this distance, vibration levels A high enough to cause fresh fracturing in the rock mass would likely be encountered, thus damaging the wall. Two options could then be contemplated, which are as follows:

1 - Modify blasting practices in order to lower the vibration equation (by reducing charge confinement, for example). This could be represented by the second curve shown on Figure 8 (dotted line). In this case, at the same distance d the vibrations anticipated would fall down to level B, which would not be sufficient to induce fresh fracturing into the rock. The cost associated with this option would be that of reducing the burden, most likely by tightening the drilling pattern.

2 - The limits of damage are inherent to a given rock mass and cannot be changed. However, the effects these limits have on the actual behaviour of the rock can be modified. Assuming again that at a distance d away from the blast fresh fracturing is likely to occur (amplitude level A), it might still be possible to prevent wall failure by putting artificial support into the ground, to prevent initial movement along these new cracks, for example. The cost associated with this second option would be that of installing this artificial ground support.

If both these steps turn out to be too expensive, then perhaps it is better to keep the design unchanged and accept the fact that the wall might be damaged by blasting. This method of superimposing a vibration prediction equation with damage limits could be another useful empirical way of taking blasting into account in the design of excavations.

Conclusions

Direct observations in the rock mass have identified three forms of blast-induced damage, which are: overbreak, creation of new fractures and extension of already existing fractures. Extension of already existing fractures was found to be the type of damage which extended the furthest from the blasted area. The creation of new cracks was restricted to a smaller zone while overbreak was usually confined to the near proximity of the blasted excavation. The onset of each type of damage could be associated, with reasonable confidence, to a vibration level. Also, the fact that vibration amplitudes could be predicted with relatively good accuracy using near-field equations, can lead to the development of a practical method to account for blasting in the design of excavations.

Future work in this field of research could use an experimental setup somewhat similar to the one

described in this paper, but in a more realistic full-size underground stope environment. The effects which different geological conditions, various stope sizes and blasting practices (mass blasting, for example), and different stress regimes have on blast-induced damage also ought to be investigated. The relationship between blast-induced damage and actual ore dilution, which is dependent upon stope geometry, stress orientation and artificial support among others, is also a challenging area for applied research.

Acknowledgements

The authors wish to thank the International Society of Explosives Engineers for the opportunity to publish this paper. Also, many thanks to all the technical and scientific personnel involved in this research program, whose dedication to the project was greatly appreciated.

Bibliography

[1] McKenzie, C., Andrieux, P., and Sprott, D., "The Significance of Amplitude in Blast Vibration Monitoring", Proceedings of the 94th Annual General Meeting of the Canadian Institute of Mining, Metallurgy and Petroleum, April 26-30, 1992, Montreal, Quebec, Canada.

[2] Holmberg, R. and Persson, P.A., "Design of Tunnel Perimeter Blasthole Patterns to Prevent Rock Damage", Proceedings of the Institute of Mining and Metallurgy Tunnelling Conference, 1979, London, England.